Numerical simulation of fiber reinforced composite materials—two procedures

E. Car [*], F. Zalamea, S. Oller, J. Miquel, E. Oñate

Departamento de Resistencia de Materiales, E.T.S. Ingenieros de Caminos, Canales y Puertos, Universidad Politécnica de Cataluña, Gran Capitán s/n Edificio C1, Campus Norte, 08034 Barcelona, Spain

Abstract

In this work, two methodologies for the analysis of unidirectional fiber reinforced composite materials are presented.

The first methodology used is a generalized anisotropic large strains elasto-plastic constitutive model for the analysis of multiphase materials. It is based on the mixing theory of basic substance. It is the manager of the several constitutive laws of the different compounds and it allows to consider the interaction between the compounds of the composite materials. In fiber reinforced composite materials, the constitutive behavior of the matrix is isotropic, whereas the fiber is considered orthotropic. So, one of the constitutive model used in the mixing theory needs to consider this characteristic. The non-linear anisotropic theory showed in this work is a generalization of the classic isotropic plasticity theory (A Continuum Constitutive Model to Simulate the Mechanical Behavior of Composite Materials, PhD Thesis, Universidad Politécnica de Cataluña, 2000). It is based in a one-to-one transformation of the stress and strain spaces by means of a four rank tensor.

The second methodology used is based on the *homogenization theory*. This theory divided the composite material problem into two scales: macroscopic and microscopic scale. In macroscopic level the composite material is assuming as a homogeneous material, whereas in microscopic level a unit volume called *cell* represents the composite (Tratamiento Numérico de Materiales Compuestos Mediante la teorí de Homogeneización, PhD Thesis, Universidad Politécnica, de Cataluña 2001). This formulation presents a new viewpoint of the homogenization theory in which can be found the equations that relate both scales. The solution is obtained using a coupled parallel code based on the finite elements method for each scale problem. © 2002 Elsevier Science Ltd. All rights reserved.

Keywords: Anisotropic; Debonding; Fiber reinforced; Homogenization theory; Composite materials; Double scale formulation; Periodic structure

1. Introduction

The use of composite materials in structures has significantly increased during the past few years. This trend is mainly because composite materials have properties which are very different from conventional

[*] Corresponding author. Tel.: +34-93-4016499; fax: +34-93-4011048.
E-mail address: car@cimne.upc.es (E. Car).

isotropic engineering materials. Composite materials present high strength–weight and high stiffness–weight ratios, are corrosion resistant, thermally stable and are well suited for structures in which the weight is a fundamental variable in the design process. Structural components requiring high stiffness and strength, impact resistance, complex shape and high volume production are suitable candidates to be manufactured using composite materials. Aerospace, automotive and marine industries are taken the advantages of the special characteristics of these materials.

Several attempts using the finite element method (FEM) for the analysis and design of composite material components have been carried out in the past few years. The correlation between analytical and measured results is deficient (Ali, 1996) (Klintworth and Macmillian, 1992). The inability to simulate the behavior of highly non-linear anisotropic materials is the main problem with conventional FEM codes. This is extremely important in fiber reinforced materials, which are strongly anisotropic.

Micro and the macro-models constitute the alternatives to study the mechanical behavior of composite materials. Micro-models focus the study at micro-mechanical level of the interatomic bounding and on the integrity of the composite beyond the damage point limit (Obraztsov and Vasilev, 1982). Although micro-models are quite expensive for practical purposes, they can be successfully used for modeling the behavior of composite materials.

Macro-models express the whole composite behavior as that of a single material. Most macro-mechanical models are based on mixing theory. This theory allows to study the behavior of composite materials as a combination of individual compounds each one with its own constitutive law satisfying an appropriate closing equation. This equation establishes the inter-material kinematics conditions. In this work, perfect compatibility between the different compounds is assumed.

The layout of the paper is the following: In the next section, the macro-model based on the mixing theory is presented. In Section 3 the constitutive model based on the homogenization theory is presented. In Section 4, an application example comparing both constitutive models is presented. Finally, the conclusions of the work are presented.

2. Macro-mechanical model

In this model and as an alternative to the "ad-hoc" models specially formulated for each compound of the composite material, relevant features about the compounding behavior are introduced through the mixing theory. It is the manager of the several constitutive laws of the different compounds and it allows to consider the interaction between the compounds of the composite materials. This theory allows to consider different type of components in the composite materials.

Trusdell and Toupin (1960) studied mixing theory providing the background for the work of Ortiz and Popov (1982a). These results also constitute the base of the work of Green and Naghdi (1965) and Ortiz and Popov (1982b) for bi-phase materials. The model presented here is a more general one and it allows to represent the non-linear constitutive behavior of a material made up of "n" anisotropic phases undergoing large strains.

In particular, in fiber reinforced composite materials the constitutive behavior of the matrix is isotropic and of the fiber is anisotropic. So, one of the constitutive model used in the mixing theory needs to consider this characteristic.

The mixing model chosen is based on the following assumptions: (i) in each infinitesimal volume of a composite material a finite number of compounding substances participate; (ii) each substance participates in the behavior of the composite in the same proportion that its volumetric participation; (iii) all compounds have the same strain (closing equation or compatibility concept); (iv) the volume occupied by each compound is much smaller than the total volume of the composite.

The second hypothesis implies a homogeneous distribution of all substances in a certain region of the composite. The interaction between the different compounding substances, each one with their own constitutive ("base") model, yields the behavior of the composite which depends on the percentage volume occupied by each substance and its distribution in the composite.

The third hypothesis is based on the fact that all phases in the mixture have the same strain field. [1] The strain compatibility condition must be fulfilled in the reference and updated configurations for each phase. On the updated configuration the condition can be written as (Trusdell and Toupin, 1960; Oñate et al., 1991):

$$e_{ij} \equiv (e_{ij})_1 = (e_{ij})_2 = \cdots = (e_{ij})_n = (\tfrac{1}{2}[I^{ij} - (b_{ij})^{-1}])_n \tag{1}$$

where e_{ij} is the Almansi strain tensor and $\boldsymbol{b} = \boldsymbol{F}\boldsymbol{F}^T$ is the left Cauchy–Green strain tensor.

In the referential configuration the closing equation proposed is:

$$E_{IJ} \equiv (E_{IJ})_1 = (E_{IJ})_2 = \cdots = (E_{IJ})_n = \tfrac{1}{2}(C_{IJ} - I_{IJ}) \tag{2}$$

where E_{IJ} is the Green–Lagrange strain tensor and $\boldsymbol{C} = \boldsymbol{F}^T\boldsymbol{F}$ is the right Cauchy–Green strain tensor.

2.1. The free energy function, stress and constitutive tensors definitions

Composite materials that fulfill Eqs. (1) and (2) also satisfy the basic condition of additivity of the free energy of their components (Trusdell and Toupin, 1960). In the updated configuration this can be expressed as

$$m\psi(\boldsymbol{e}^e, \theta, \alpha^m) = \sum_{c=1}^{n} k_c m_c \psi_c \left[\boldsymbol{e}, (\boldsymbol{e}^p)_c, \theta, \alpha_c^m \right] \tag{3}$$

where m and m_c are the density of the composite and of each of the phases in the updated configuration, respectively, ψ_c the free energy corresponding to each one of the compounding substances of the mixture, k_c the volumetric participation coefficient, $(\boldsymbol{e}^p)_c$ the plastic deformation of each phase and α_c^m are the internal variables of each phase, which define the physical behavior of the phase.

The definition of the stress $\boldsymbol{\tau}$ of the whole composite is obtained considering an hyperelastic model (Malvern, 1969) as

$$\boldsymbol{\tau} = m\frac{\partial \psi}{\partial \boldsymbol{e}} = \sum_{c=1}^{n} k_c m_c \frac{\partial \psi_c}{\partial \boldsymbol{e}} = \sum_{c=1}^{n} k_c (\boldsymbol{\tau})_c \tag{4}$$

where k_c is the ratio between the volume of the compounding c and the total volume of the whole composite. The elastoplastic tangent constitutive tensor is obtained as (Car et al., 2000)

$$\boldsymbol{c}^T = \frac{\partial^2 \psi}{\partial \boldsymbol{e} \otimes \partial \boldsymbol{e}} = \sum_{c=1}^{n} k_c (\boldsymbol{c}^T)_c \tag{5}$$

where $(\boldsymbol{c}^T)_c$ is the tangent elastoplastic real anisotropic constitutive tensor. Details of the derivation of the elastoplastic tensor are given in Oller et al., 1996.

---

[1] This assumption is valid in absence of atomic diffusion. The atomic diffusion phenomena take place at high temperatures. In this analysis a moderate temperature below melting point is considered.

2.2. Large strain elastoplastic anisotropic model

2.2.1. Material formulation

Fibre reinforced composite materials are made, basically, with two phases: matrix and fiber. The constitutive model is based on the mixing theory of basic substance acting as a manager of the constitutive laws of the matrix and fiber phases and it allows to consider the interaction between these phases. In fiber reinforced composite materials, the constitutive behavior of the fiber is anisotropic.

The anisotropic theory developed in this work is based on the ideas proposed by Betten (Betten, 1981, 1988) and uses the concept of *mapped tensors*. This concept allows to use the advantages and algorithms developed for classic isotropic materials. The implementation of this theory in finite element codes is straightforward. The anisotropic behavior of the material is expressed in terms of isotropic fictitious stress and strain spaces, which are the linear tensor transformations of the real anisotropic stress and strain spaces. All the information on the material anisotropy is contained in the fourth order transformation tensors A^S and A^E in the reference configuration and a^τ and a^e in the updated configuration relating the stresses and strains in the real (anisotropic) and fictitious (isotropic) spaces. The parameters that define the transformation tensors in the reference configuration can be calibrated from adequate experimental tests. Under large strain hypothesis, a^τ and a^e in the updated configuration, are obtained considering the deformation gradient (Car et al., 2001). The constitutive model in the fictitious isotropic space is defined by the same yield function, plastic potential and integration algorithms developed for standard isotropic materials.

The transformation of the second Piola–Kirchhoff stress tensor S in the anisotropic space to the isotropic space is performed by:

$$\overline{S}_{IJ} = A^S_{IJKL} S_{KL} \tag{6}$$

where A^S is a four rank tensor which relates the stress tensors in the real and fictitious spaces, $\overline{S}$ and S are the second Piola–Kirchhoff stress tensor in the fictitious isotropic and real anisotropic stress spaces respectively. The four rank tensor A^S is defined in the reference configuration and remains constant in this configuration. The definition of the elements of A^S is obtained considering the symmetry of the Cauchy stress tensor in the anisotropic and isotropic spaces, therefore the four rank transformation tensor must satisfy the following symmetries:

$$A^S_{ijkl} = A^S_{jikl} = A^S_{jilk} \tag{7}$$

The symmetry of the four rank transformation tensors is also necessary:

$$A^S_{ijkl} = A^S_{klij} \tag{8}$$

The global expression of A^S is obtained by standard transformation of the local components given by

$$A^S_{IJKL} = R_{IJRS}(A^S_{RSPQ})_{\text{loc}} R_{PQKL} \tag{9}$$

where $(A^S_{RSPQ})_{\text{loc}}$ is the four rank stress transformation tensor in the local coordinate system and R is a rotation matrix.

It is also necessary to define the relationship between the Green–Lagrange elastic strain in the real anisotropic space E^e and the Green–Lagrange elastic strain $\overline{E}^e$ in the fictitious isotropic space. This relation is

$$\overline{E}^e_{IJ} = A^E_{IJKL} E^e_{KL} \tag{10}$$

where A^E is a four rank tensor, which relates the Green–Lagrange strains in the anisotropic and isotropic spaces, $\overline{E}$ and E are the Green–Lagrange strain tensors on the isotropic space and anisotropic space respectively. The four rank strain transformation tensor is computed taking into account Eqs. (6) and (10)

$$A_{MNRS}^E = \left(\overline{C}_{MNIJ}\right)^{-1} A_{IJKL}^S C_{KLRS} \tag{11}$$

where $\overline{C}_{MNIJ}$ is the constitutive tensor in the isotropic space and C_{KLRS} is the constitutive tensor in the real anisotropic space. The choice of $\overline{C}_{MNIJ}$ can be arbitrary and for this purpose the properties of any known material can be chosen, because their influence in the computations is cancelled when all the quantities are returned to the real space.

The anisotropic constitutive tensor $\boldsymbol{C}$ is defined in global axes by the following transformations

$$C_{IJKL} = R_{IJRS}\left(C_{RSPQ}\right)_{\text{loc}} R_{PQKL} \tag{12}$$

where $\left(C_{RSPQ}\right)_{\text{loc}}$ is the local four rank constitutive tensor in the anisotropic space in the local coordinate system and $\boldsymbol{R}$ is a rotation matrix.

2.2.2. Updated formulation

The relationship between the Kirchhoff stresses in the anisotropic and isotropic spaces on the updated configuration is given by

$$\overline{\tau}_{ij} = a_{ijkl}^\tau \tau_{kl} \tag{13}$$

where $\boldsymbol{a}^\tau$ is the four rank tensor, which relates the stress tensor in the anisotropic and isotropic spaces on the updated configuration, $\overline{\tau}$ and τ are the Kirchhoff stress tensors in the isotropic and anisotropic spaces respectively.

In a large strain context, it is necessary to redefine the four rank transformation tensor on the updated configuration due to the fact that the four rank tensor $\boldsymbol{a}^\tau$ is not constant in this configuration and it is a function tensor $\boldsymbol{A}^S$ in the referential configuration and the deformation gradient $\boldsymbol{F}$. Tensor $\boldsymbol{a}^\tau$ in the updated configuration is obtained by the "push-forward" operations (Car et al., 2000):

$$a_{ijkl}^\tau = F_{iI}\left(F^{-1}\right)_{Kk}\left(F^{-T}\right)_{lL}\left(F^T\right)_{Jj} A_{IJKL}^S \tag{14}$$

Similarly, the relation between Almansi strains in the anisotropic and isotropic spaces is defined by

$$\overline{e}_{ij} = a_{ijkl}^e e_{kl} \tag{15}$$

where tensor $\boldsymbol{a}^e$, establishes the relationship between the Almansi strain tensors in the anisotropic and isotropic spaces and $\overline{e}$ and e are the Almansi strain tensors in the anisotropic and isotropic spaces respectively.

In a similar way $\boldsymbol{a}^e$ on the updated configuration is obtained as:

$$a_{ijkl}^e = \left(F^{-T}\right)_{iI}\left(F^T\right)_{Kk} F_{lL}\left(F^{-1}\right)_{Jj} A_{IJKL}^E \tag{16}$$

In Fig. 1, the four rank tensors which relate the stresses and strains spaces in the real and fictitious spaces in the referential ($\boldsymbol{A}^S$ and $\boldsymbol{A}^E$) and updated ($\boldsymbol{a}^\tau$ and $\boldsymbol{a}^e$) configurations are shown.

2.2.3. Flow rule and evolution law for the internal variables

The evolution law of the plastic deformation on the updated configuration is given by:

$$L_v\left(\boldsymbol{e}^p\right) = \boldsymbol{d}^p = \dot{\lambda}\frac{\partial g}{\partial \boldsymbol{\tau}} \tag{17}$$

Taking into account that all the information on the material anisotropy is contained in the four rank transformation tensor $\boldsymbol{a}^\tau$, the following plastic potential function on the fictitious space is proposed

$$g(\boldsymbol{\tau}; \boldsymbol{g}; \alpha) = \overline{g}(\boldsymbol{\tau}; \boldsymbol{a}^\tau; \boldsymbol{g}; \alpha) = \overline{g}(\overline{\boldsymbol{\tau}}; \boldsymbol{g}; \alpha) = k \tag{18}$$
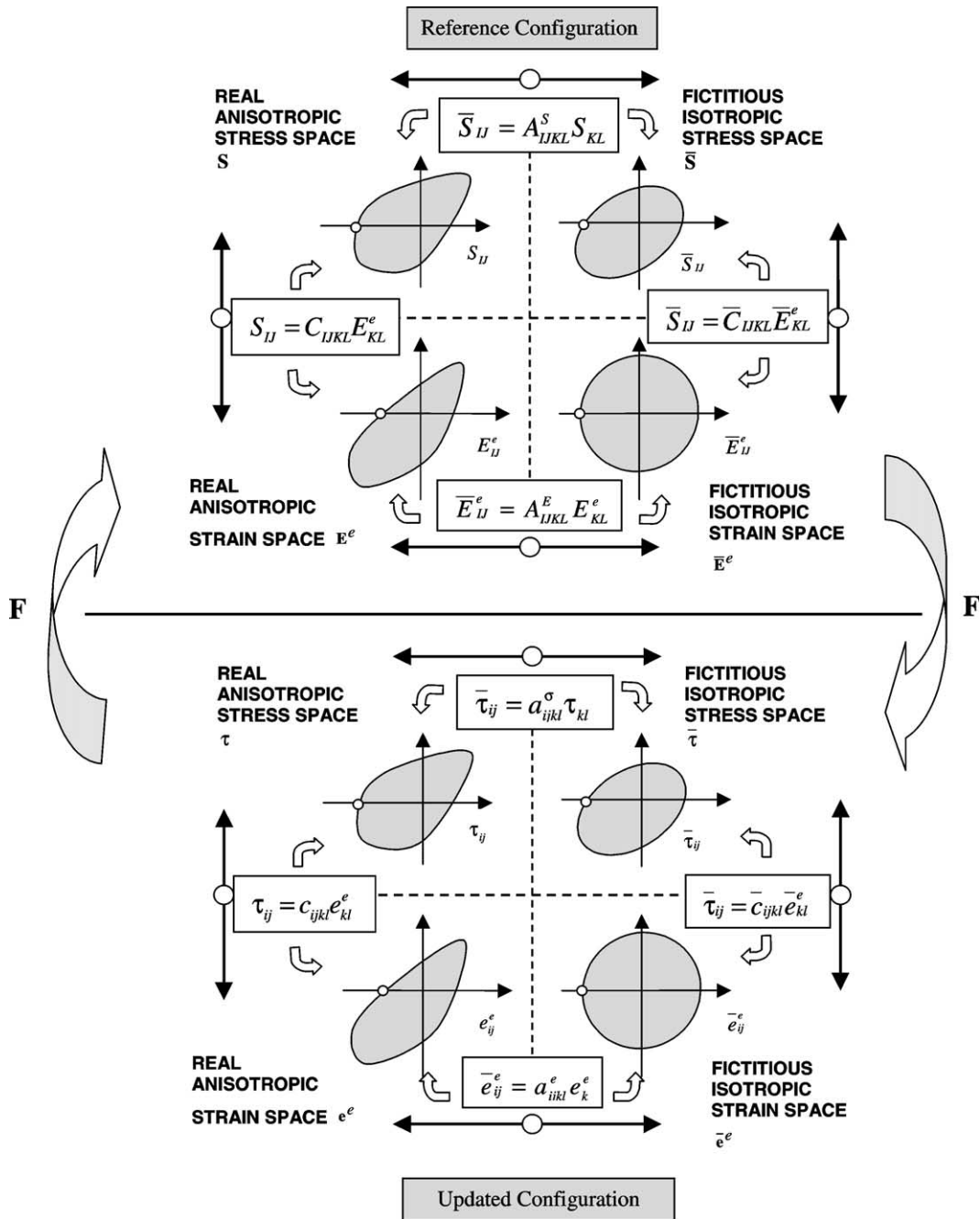
Fig. 1. Extension of the anisotropic model to large strains. Spaces definition in reference and updated configurations.

Considering Eqs. (17) and (18) the evolution of the plastic part of Almansi strain is

$$\boldsymbol{d}^p = \dot{\lambda}\frac{\partial g}{\partial \boldsymbol{\tau}} = \dot{\lambda}\frac{\partial \overline{g}}{\partial \overline{\boldsymbol{\tau}}} : \frac{\partial \overline{\boldsymbol{\tau}}}{\partial \boldsymbol{\tau}} = \dot{\lambda}\frac{\partial \overline{g}}{\partial \overline{\boldsymbol{\tau}}} : \boldsymbol{a}^\tau = (\dot{\overline{\boldsymbol{e}}})^\tau : \boldsymbol{a}^\tau \tag{19}$$

where $(\dot{\bar{\boldsymbol{e}}})^\tau$ is the plastic flow normal to the plastic potential function $\overline{g}$ in the isotropic space. The additivity concept of the strain velocity allows to extend the strain transformation rule to the plastic part of the strains, so

$$\overline{\boldsymbol{d}}^p = \boldsymbol{a}^e : \boldsymbol{d}^p = \dot{\lambda}\boldsymbol{a}^e : \frac{\partial \overline{g}}{\partial \overline{\boldsymbol{\tau}}} : \boldsymbol{a}^\tau = \boldsymbol{a}^e : (\dot{\bar{\boldsymbol{e}}})^\tau : \boldsymbol{a}^\tau \tag{20}$$

where $\overline{\boldsymbol{d}}^p$ is the isotropic plastic strain on the updated configuration. The evolution of the plastic hardening internal variable is given by

$$\dot{\alpha} = \dot{\lambda}(\boldsymbol{h}^m)_\sigma : \frac{\partial g}{\partial \tau} = \dot{\lambda}(\boldsymbol{h}^m)_\sigma : \frac{\partial \overline{g}}{\partial \overline{\boldsymbol{\tau}}} : \frac{\partial \overline{\boldsymbol{\tau}}}{\partial \tau} = \dot{\lambda}(\boldsymbol{h}^m)_\sigma : \frac{\partial \overline{g}}{\partial \overline{\boldsymbol{\tau}}} : \boldsymbol{a}^\tau \tag{21}$$

where the second order tensor $(\boldsymbol{h}^m)_\sigma$ is a function of the actual stress state and of the actual hardening plastic variable. This tensor, in the simplest case of plasticity theory, is the stress tensor. Therefore, the evolution law of the internal variable is written as

$$\dot{\alpha} = \dot{\lambda}\overline{\boldsymbol{\tau}} : \frac{\partial \overline{g}}{\partial \overline{\boldsymbol{\tau}}} \tag{22}$$

2.3. Debonding phenomenon

The compatibility equation in the updated and in the referential configuration (Eqs. (1) and (2)) is suitable only for composite materials with parallel behavior. The stress in the whole composite material is obtained considering that all the substances contribute to the behavior of the composite proportionally to the relative volume that they occupy, ex.: reinforced concrete, long fiber reinforced composite materials, etc.

Due to the presence of other phenomena in the failure of composite materials, the classical mixing theory is not enough, i.e. short fiber reinforced composite materials or debonding phenomena. This phenomenon takes place in composite materials when there is a relative slip between compounding and the maximum shear stress of the interface is greater than its yield value. In this case, the matrix is not able to transfer the loads to the fiber, so the fiber cannot increase its stress state because the matrix–fiber interface cannot resist it. The modification in the mixing theory to take into account these phenomena is based on the ideas that the transfer of loads between matrix and fiber change when the matrix plastifies. This model is considered a "*non-local material*" model. It is based on defining the stress state in the fiber at the time the matrix reaches the plastic state. Then the fibers increase their stress state according to a new constitutive tensor, which is a function of the frictional forces between matrix and fibers. Due to the load transmission mechanism between matrix and fiber, the maximum strength of the fiber is given by (Car, 2000)

$$\left(f_\tau^R\right)_{\mathrm{Fib}} = \min\left\{\left(f_\tau^N\right)_{\mathrm{Fib}}, \left(f_\tau^N\right)_{\mathrm{Mat}}, 2\left(f_\tau^N\right)_{\mathrm{Fib-Mat}}/r_f\right\} \tag{23}$$

where $\left(f_\tau^N\right)_{\mathrm{Fib}}$, $\left(f_\tau^N\right)_{\mathrm{Mat}}$ and $2\left(f_\tau^N\right)_{\mathrm{Fib-Mat}}/r_f$ are the nominal shear strength of the fiber, matrix and fiber–matrix interface (Car, 2000).

As it has been seen in this section, the classical mixing theory has strong limitations to represent the behavior of composite materials whose compounds do not participate in a parallel way. Nevertheless the adjustment in the classical mixing theory made in this work allows to approach the complex phenomenon which could not be take into account with the classical mixing theory. The quality of the modified theory here presented could be see in the comparison with the results obtained with experimental tests.

3. Homogenization theory

The homogenization theory is an alternative formulation to simulate the constitutive behavior of composite materials. Various multi-scale methods have been developed to resolve the problems presented by composite materials. These methods can be included in the context of the *homogenization theory*, in which the composite material problem is divided into two different scales. Thus, the composite material is assumed to be homogeneous material on a *macroscopic scale* (x_i) and its behavior can be studied by taking a representative unit volume, represented on a second scale (y_i), called *microscopic scale*. When the internal structure of the composite material is periodic, the representative unit volume is called a *cell*. The use of these two scales is equivalent to determining the properties of a given composite material under a limiting condition, i.e. when the cell's dimensions tend toward zero.

The *homogenization theory*, proposed and developed by Sanchez-Palencia (Sanchez-Palencia, 1980), Bensoussan (Bensoussan et al., 1978), Duvaut (Duvaut, 1976), is formulated in terms of the *asymptotic expansion theory*. On the other hand, Suquet (Suquet, 1982, 1987) employs the *method of averages* and finds that upon extending it to the non-linear case, the macroscopic variables become coupled to the respective microscopic ones. This presents an important difficulty because coupling implies that the composite constitutive equation depends on an ''infinite number of internal variables''. For the purposes of obtaining a simplified constitutive law for the composite, it has been proposed to make certain simplifications, however, these are only applicable to simpler structural problems. In recent years, various methods have been proposed as a solution to the non-linear two scale problems. (Ghosh et al., 1996) proposes a no-conventional method in which the composite microstructure is represented by *finite Voronoi elements* and used the asymptotic expansion theory as a bridge between the two scales. Fish (Fish et al., 1997), on the other hand, uses the *field transformation theory* (Dvorak et al., 1994) as well as the asymptotic expansion theory. In any case, use of these methods seeks to reduce computational effort, but can however, result in a certain loss of accuracy.

This paper uses a double-scale method formulation (Zalamea, 2001). This formulation is based on previous concepts developed in foregoing formulations, especially by the local periodicity vectors. Following the classical double scale method and thanks to the analysis of the periodical media behavior, it is possible to obtain the government equation for each one of the macroscopic and microscopic scale levels. In this formulation no second order terms are needed in order to represent the periodic fluctuations on the microscopic level, such as that shown in the classical asymptotic developments.

In the developed equations, the *homogenized strain tensor* (macroscopic strain tensor) is obtained throughout the change of the symmetries in the media. These symmetries are represented by means of the so called periodicity vectors. The *homogenized stress tensor* (macroscopic stress tensor) is the result of the symmetries of the forces in the cell boundary and represents the average of the microscopic stresses generated in the cell domain. With these connections, in the stresses and strains field, the composite material problem can be formulated in each one of the two scales and their solutions can be obtained by numerical coupling using the FEM. In the following section a brief synthesis of the formulation used herein will be presented.

3.1. Formulation of the homogenization theory

Given a body in a global system of references X and assuming that this body is made up of a fine periodic structure domain that its only be appreciated by amplifying a small domain, in that case, we can use a microscopic coordinate system Y which would be sensitive to extremely small dimensions, see Fig. 2.

All periodic composite materials are, in fact, heterogeneous media which have one or more translation symmetries. These symmetries can be represented by vectors that define the exact locations of the particles
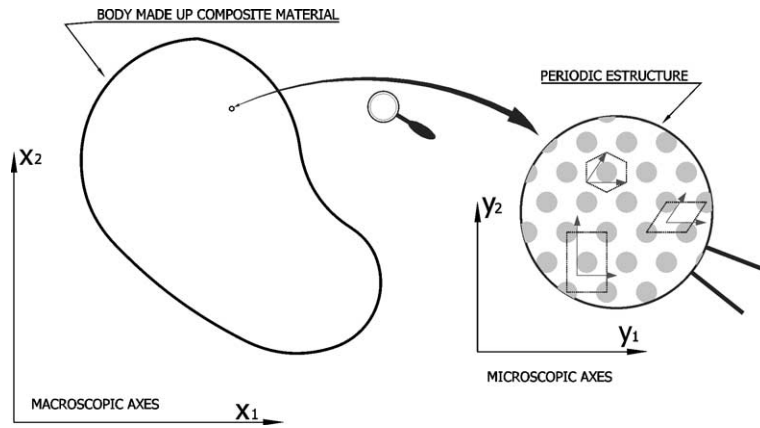
Fig. 2. Two scales representation, macroscopic and microscopic.

or points which necessarily have equal properties. Therefore, each point of the continuum media belongs to a group of points, called *periodic points*.

The periodic distribution of the constituent materials creates symmetries which permits splitting the composite materials into structural units called *cells*. This virtual split of the medium is achieved by means of parallel surfaces called *sides* which satisfies the translation symmetry. Thus, a composite material represented as a two-dimensional space, can be divided into four sided cells (two pairs of periodic sides) called *quadrilateral cell*, or into cells of six sides (three pairs of periodic sides) called *hexagonal cells*.

The points in which the material coordinates Y_i have the same relative position in the neighboring cells, are called *periodic points*; e.g. in Fig. 3, a point whatever in the cell domain is indicated by P; in the neighboring cells these same points (P) have been so indicated; these are the so called periodic points.

The relative position of these points determine a base of vectors D_i which are the *periodicity vectors*. Therefore, each point on the cell boundary has a periodic point on the opposite side. Moreover, in quadrilateral cells, the four corners are periodic whilst in hexagonal cells, the six corners divide into two groups of three periodic points.
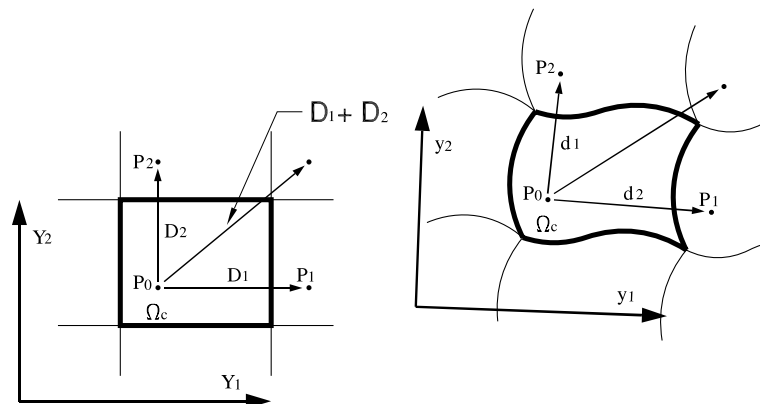

Fig. 3. Periodicity vectors in the referenced configuration D_i and the new periodicity vectors d_i on the up-dated configuration.

3.2. The relationship between the scales

For heterogeneous material, some concepts such as stress or strain can be understood as values that are dependant upon the scale. For example: seen macroscopically, the composite material may be considered as a homogeneous material in which each point has an effective stress or strain value. Nevertheless, at the microscopic level, there can be great fluctuations in the values of these variables. In passing from the microscopic variables to the macroscopic ones, the hypothesis of *local periodicity* (Sanchez-Palencia, 1987) is used. This hypothesis is a consequence of energy minimization, which ordains that the microscopic variables within the cell are equal to the respective variables of neighboring cells, but may be very different from those cells that are more distant.

3.2.1. The homogenized strain tensor

Considering that Ω_c represents a cell domain of a composite material (represented in material space Y_i), and this cell domain is characterized by the periodicity vector $\boldsymbol{D}_i$ ($\boldsymbol{D}_i = \boldsymbol{Y}_{p_i} - \boldsymbol{Y}_{p_0}$). Then if the medium undergoes a displacement, the local periodicity hypothesis ensures that composite material, despite its deformation, retains its periodicity relation with its neighboring cells. Therefore, the deformed cell, together with its neighboring cells, all undergoes the same transformation. Consequently, the new periodicity vectors d_i can be written as

$$\boldsymbol{d}_i = \boldsymbol{y}_{p_i} - \boldsymbol{y}_{p_0} = \boldsymbol{D}_i + (\boldsymbol{u}_{p_i} - \boldsymbol{u}_{p_0}); \quad i = 1, 2 \tag{24}$$

where, $\boldsymbol{u}_{p_i} - \boldsymbol{u}_{p_0}$ is the displacement difference between periodic points. The transformation of the cells space is associated with the change of periodicity vectors. The partial derivative of these vectors is

$$\frac{\partial \boldsymbol{d}_i}{\partial \boldsymbol{D}_j} = \frac{\partial (\boldsymbol{y}_{p_i} - \boldsymbol{y}_{p_0})}{\partial (\boldsymbol{Y}_{p_j} - \boldsymbol{Y}_{p_0})} \tag{25}$$

Now then, on the macroscopic level, the periodicity vectors are infinitesimally small ($|\boldsymbol{D}| \to 0$). Consequently, on a macroscopic scale this value tends toward a limit

$$\lim_{D \to 0} \left(\frac{\partial \boldsymbol{d}_i}{\partial \boldsymbol{D}_j} \right) = \lim_{D \to 0} \left[\frac{\partial (\boldsymbol{y}_{p_i} - \boldsymbol{y}_{p_0})}{\partial (\boldsymbol{Y}_{p_j} - \boldsymbol{Y}_{p_0})} \right] = \frac{\partial \boldsymbol{x}}{\partial \boldsymbol{X}} = \boldsymbol{F} \tag{26}$$

then,

$$\boldsymbol{d} = \boldsymbol{F}\boldsymbol{D}$$

where $\boldsymbol{F}$ is the *homogenized deformation gradient tensor*. This simple change of scale allows to obtain the macroscopic strain tensor using the classical mechanics of continuous mediums. The square of the length of the new periodicity vectors is

$$|\boldsymbol{d}|^2 = \boldsymbol{D}^T (\boldsymbol{F}^T)(\boldsymbol{F}) \boldsymbol{D} \tag{27}$$

and the difference between the square of the length of the new periodicity vectors and the periodicity vectors in the reference configuration is

$$|\boldsymbol{d}|^2 - |\boldsymbol{D}|^2 = [\boldsymbol{D}^T \boldsymbol{F}^T][\boldsymbol{F}\boldsymbol{D}] - \boldsymbol{D}^T \boldsymbol{D}$$
$$|\boldsymbol{d}|^2 - |\boldsymbol{D}|^2 = 2\boldsymbol{D}^T \boldsymbol{E} \boldsymbol{D}. \tag{28}$$

Thus, the Green Lagrange tensor expressed in Eq. (2) is obtained here as a measure of strain on a macroscopic scale

$$E = \frac{1}{2}\left[F^T F - I\right] = \frac{1}{2}\left[\frac{\partial d^T}{\partial D}\,\frac{\partial d}{\partial D} - I\right] \tag{29}$$

This tensor E can be called *homogenized strain tensor* and is associated with the change of periodicity vectors. This equation means that if the medium has local periodicity, the strain is measured by the change of position between periodic points. This measurement is independent of the periodical fluctuations in the cell boundary. For example, assuming a continuum media under periodic displacements field, in which the periodicity vectors remain without changes because the relative position among the "constant" points (Fig. 4), and in spite of the oscillation of the microscopic strains, the macro-scale strains remain zero. In opposition, if some periodicity vector is modified, a strain phenomenon takes place in the micro-scale and it is amplified to the macro-scale.

Eq. (26) does not have terms that represent the periodic part. This is due to that the change of the periodicity vectors defines the change between periodic points. This change is independent of the periodic fluctuations that take place.

Notice that in this case, contrary to other procedures (classical asymptotic expansion theory) the second order strain terms are not used to determine the periodic part. Eq. (29) allows establish a condition in the displacement field, necessary to solve the boundary value problem at the cell level. From here the microscopic strain field is obtained. Moreover, it coincides with the classical equation of the *average theory* (Suquet, 1982)

$$E = \langle \varepsilon(y)\rangle_{\Omega_c} = \frac{1}{\Omega_c}\int_{\Omega_c}\varepsilon(y)\,d\Omega_c \tag{30}$$

where, ε is the *microscopic strain field* and Ω_c is the cell domain.

3.2.2. The homogenized stress tensor and the equilibrium equation

Consider Ω as a domain of a composite material with a periodic distribution of its compounds. This domain is divided into cells, whose volume V_c is very small macroscopically ($V_c \to 0$). Then, disregarding the
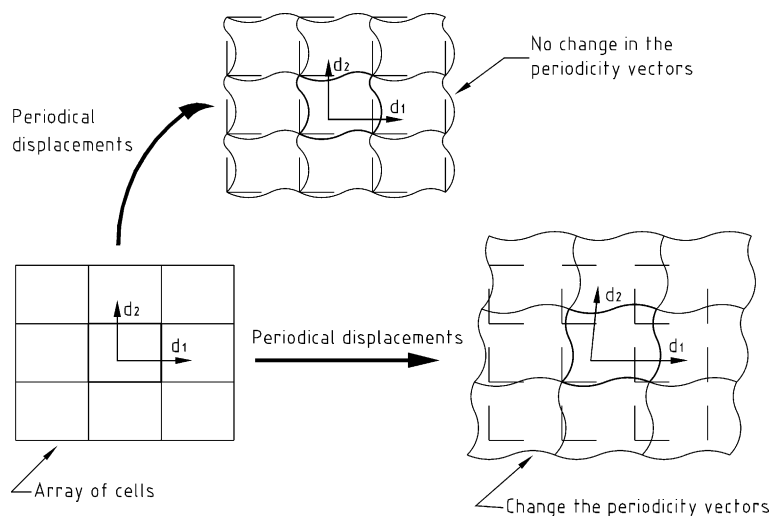

Fig. 4. Periodicity vectors in the referenced configuration D_i and the new periodicity vectors d_i on the updated configuration.

effect of the volume forces (on a microscopic scale), the static equilibrium equation on the cell domain is

$$\int_{S_c} \sigma_{ij} n_j \, dS_c = 0 \tag{31}$$

where, S_c is the boundary surface of the cell, $\boldsymbol{\sigma}$ is the microscopic stress field, $\boldsymbol{n}$ is a unit normal vector of the surface element dS. The orientation of two surface elements located at periodic points (see Fig. 5) has unit normal vectors ($\boldsymbol{n}_1$ and $\boldsymbol{n}_2$) in opposite directions. Due to equilibrium conditions the surface forces $\boldsymbol{F} = \boldsymbol{t}(\boldsymbol{n}) \, dS_c$ in the two surface elements are equal but with opposite direction. This is known in the homogenization literature as an anti-periodic force field (Lene, 1986) on the cell's sides.

A second order tensor Σ_{ij} is defined as the average of the forces acting on the cell's sides:

$$\Sigma_{ik} = \frac{\int_{S_c} y_k \sigma_{ij} n_j \, dS_c}{\int_{S_c} y_k n_j \, dS_c} \tag{32}$$

If the volume forces effect is disregarded ($\sigma_{ij,j} = 0$), and using the divergence theorem, the average theory equation is obtained:

$$\Sigma_{ik} = \frac{\int_{V_c} y_{k,j} \sigma_{ij} \, dV_c}{\int_{V_c} y_{k,j} \, dV_c} = \frac{\int_{V_c} \delta_{k,j} \sigma_{ij} \, dV_c}{\int_{V_c} \delta_{k,j} \, dV_c} = \frac{1}{V_c} \int_{V_c} \sigma_{ik} \, dV_c \tag{33}$$

The *overall surface force* $\widetilde{\boldsymbol{t}}(\hat{\boldsymbol{n}})$ is defined as the average of the forces on the cell sides S_c determined by the direction of a (macroscopic) unit vector $\hat{\boldsymbol{n}}$,

$$\widetilde{t}_i(\hat{\boldsymbol{n}}) = \frac{\int_{S_c} y_k \sigma_{ij} n_j \, dS_c}{\int_{S_c} y_k n_j \, dS_c} \hat{n}_k = \frac{1}{V_c} \int_{V_c} \sigma_{ik} \, dV_c \hat{n}_k \tag{34}$$

The value of the right hand side of the equation is a linear function that depends on the direction of $\hat{\boldsymbol{n}}$ (i.e. $\widetilde{t}_i(\hat{\boldsymbol{n}}) = \Sigma_{ik}\hat{n}_k$), and since the tensor $\boldsymbol{\Sigma}$ fulfils, on the macroscopic level, the same requirements of the stress tensor $\boldsymbol{\sigma}$ (on homogeneous materials), the tensor $\boldsymbol{\Sigma}$ is henceforth called the *homogenized stress tensor*.

On the other hand, if the whole composite material's domain Ω (which is formed by an infinite number of cells) is considered, the static equilibrium equation can be written as:

$$\int_S \left(\frac{1}{V_c} \int_{V_c} \sigma_{ij} \, dV \right) \hat{n}_j \, dS + \int_V \left(\frac{1}{V_c} \int_{V_c} \rho b_i \, dV_c \right) dV = 0 \tag{35}$$
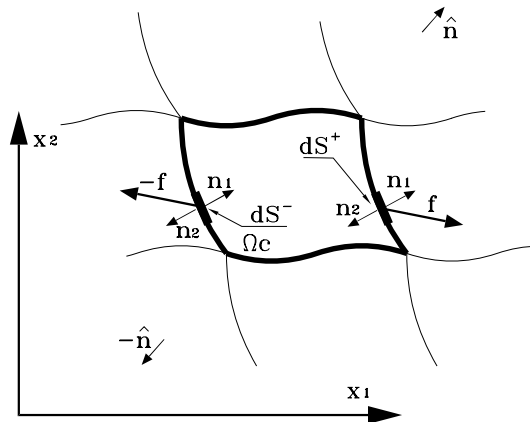

Fig. 5. Acting forces on the cell boundaries.

The body forces per unit volume must be considered because on a macroscopic scale their magnitudes can be important. This effect may be assumed as the average of the volume forces ($\widetilde{\boldsymbol{b}}$) inside the cell, or

$$\widetilde{b}_i = \frac{1}{V_c} \int_{V_c} \rho b_i \, dV_c = \text{constant} \tag{36}$$

substituting Eqs. (33) and (36) in Eq. (35) and using the divergence theorem,

$$\int_V \Sigma_{ij,j} \, dV + \int_V \widetilde{b}_i \, dV = 0 \tag{37}$$

This equation is valid for an arbitrary volume V and, therefore, it is valid when choosing very small domains (the limit of which is the cell domain ($\Omega \to \Omega_c$; $\Omega_c \to 0$)), then

$$\Sigma_{ij,j} + \widetilde{b}_i = 0 \tag{38}$$

and thus we obtain the *homogenized local equation of static equilibrium* is obtained.

3.3. Formulation of the problem in each scale

Consider a body, which occupies a region Ω formed by a composite material of fine periodic structure. The boundary of Ω is noted $\partial\Omega$ in which $\partial\Omega_u$ is the part of the boundary where the displacements are known (Dirichlet's conditions) and $\partial\Omega_t$ is the part of the boundary where the surface forces are known (Newman's condition). On the other hand, the structure of this material lends itself to being divided into very small structural units (cells). This domain is a space Ω_c such that, by ordered repetition the body of the composite material Ω can be restored. Moreover, two scales of differing orders of magnitude are assumed in such a way that the particles of the domain Ω can be labeled in accordance with their position within a space x_i (at a macroscopic level), while the position of the cell's particles can be labeled within a local space y_i (at a microscopic level). Therefore, at a macroscopic level, the problem of composite materials becomes a boundary-value problem of homogeneous materials in which we look for displacement and stress fields $(\boldsymbol{u}(x), \boldsymbol{\Sigma}(x))$, which satisfy the following equations:

$$\frac{\partial \boldsymbol{\Sigma}(x)}{\partial \boldsymbol{x}} + \widetilde{\boldsymbol{b}} = 0 \quad \text{equilibrium equation in } \Omega \tag{39}$$

$$\boldsymbol{\Sigma}(x) = \frac{1}{\Omega_c} \int_{\Omega_c} \boldsymbol{\sigma}(x,y) \, d\Omega_c \quad \text{constitutive equation in } \Omega \tag{40}$$

$$\boldsymbol{u}(x) = \bar{\boldsymbol{u}}(x) \quad \text{displacements on } \partial\Omega_u \tag{41}$$

$$\boldsymbol{\Sigma}(x) : \boldsymbol{n} = \bar{\boldsymbol{t}}(x) \quad \text{forces on } \partial\Omega_t \tag{42}$$

On the other hand, at the microscopic level, the cell's boundary conditions must locally reproduce the conditions of the material microstructure. Then, in accordance with the local periodicity hypothesis, when the composite material is subjected to a microscopic deformation, the change in the periodicity vectors is described by

$$\boldsymbol{d}_i - \boldsymbol{D}_i = \boldsymbol{u}_{p_i} - \boldsymbol{u}_{p_0} \tag{43}$$

in which $\boldsymbol{u}_{p_i}$ and $\boldsymbol{u}_{p_0}$ represents the displacements of two periodic points, $\boldsymbol{D}_i$ represents the periodicity vector defined between these points in the microscopic reference configuration X_i, and $\boldsymbol{d}_i$ is the new periodicity vector came out from the deformation. Under small-strains hypothesis, the relative displacement between

the cell boundary's periodic points is equivalent to (Zalamea et al., 1999):

$$\boldsymbol{u}_{p_i} - \boldsymbol{u}_{p_0} \simeq \boldsymbol{E}\boldsymbol{D}_i \tag{44}$$

This relative displacement condition between boundary points represents a field of periodic displacements. Additionally, the forces generated in the cell boundary are of equal magnitude but have opposite directions. Then, the problem on a microscopic scale, y_i, comes down to solving the following boundary-value problem in the cell domain Ω_c:

$$\frac{\partial \boldsymbol{\sigma}(y)}{\partial \boldsymbol{y}} = 0 \quad \text{equilibrium equation in } \Omega_c \tag{45}$$

$$\dot{\boldsymbol{\sigma}}(y) = \boldsymbol{C}(y) : \dot{\boldsymbol{\varepsilon}}(y) \quad \text{constitutive equation in } \Omega_c \tag{46}$$

$$\boldsymbol{u}_{p_i} - \boldsymbol{u}_{p_0} = \boldsymbol{E}\boldsymbol{D}_i \quad \text{periodic displacements on } \partial\Omega_c \tag{47}$$

$$\boldsymbol{t}_{p_i} = -\boldsymbol{t}_{p_0} \quad \text{periodic forces on } \partial\Omega_c \tag{48}$$

where Eq. (45) is the microscopic static equilibrium equation (disregarding the effect of the volume forces); this equation must hold for each point of the cell domain. The behavior of the compounding materials is represented by the expression 46 in which $\boldsymbol{C}$ is the constitutive tensor. In this case, the constitutive equation of compounds materials may be of any kind (elastic, plastic, viscous, etc.). Eqs. (47) and (48) create displacement and force periodicity conditions in the boundary of the cell $\partial\Omega_c$, and at the same time connect, through the strain tensor $\boldsymbol{E}$, with the local state at the macroscopic level. Consequently, both problems are interrelated, i.e. the solution of the problem on a macro-scale requires that each point of the domain Ω satisfies the microscopic boundary-value problem (Eqs. (45)–(48)); this implies an infinite number of problems at the microscopic level. However, despite the difficulty implied, this problem can be solved in a discrete way by use of the FEM.

3.4. Macro–micro-structural coupling

For the solution of the problems concerning composite materials by the homogenization method, a macro–micro-structural coupling is proposed using the FEM in two scales (see Ghosh et al. (1996) and Fish et al. (1997) for other coupling two-scale methods). Then, on the macroscopic scale we look for equilibrium forces in the composite material's body, whereas on the microscopic scale we determine the behavior of the composite material. Thus, each integration point of the macro-structure's finite element represents a boundary-value problem on the microscopic scale. This means that the law governing the composite material's behavior is a numerical constitutive equation. In this case, this macroscopic law is *strain-driven* (by means of the boundary condition imposed on the cell). The internal variables of the composite material correspond to all of the internal variables in the whole cell domain. Then, in the global problem one must simultaneously solve the macro-structure and as many cells (of the composite material) as the number of integration points that the macro-structure contains. The solution is obtained once all the boundary-value problems satisfies the equilibrium equations.

The finite element implementation of two-scales problem is carried out using *Parallel Virtual Machine* (PVM) (Geist et al., 1994). This software creates a virtual data processing system constituted by one or more computers in which several processes are handled at the same time. Then, one process solves the macroscopic problem whereas one or more parallel processes solve the problems at the microscopic level. These processes are synchronized and they exchange information when necessary. Inasmuch as each of the boundary-value problems on a microscopic scale is an independent problem, this implementation allows to solve the cell problems in one or in as many processors available.

4. Example

In this section, an application example using the proposed model is presented. The examples consist in the numerical simulation of the non-linear behavior of a specimen made up of composite material subjected to a tension state. The simulations have been carried out using a finite element mesh of standard four node rectangular finite elements with 548 elements, 603 nodes and 1124 degrees of freedom. This mesh is similar to the one used in a study carried out by the European Space Agency (Stavrinidis, 1985).

The test is carried out on specimens of carbon-epoxi T300/914C that present a notch in the central area of the specimen. The reinforcement are carbon fibers. The angle orientations of the carbon fibers in the different tests specimens is 0° related to the longitudinal axis of the sample.

The test consists in a tensional state imposing a displacement on the top of the specimen. In Fig. 6 dimensions of the specimen, a detail of the central area and the points in which the experimental measures were carried out are observed.

In the notched area a stress concentration is generated which perturbs the matrix. This situation generates stresses that exceed the elastic limit of the matrix. In unidirectional fiber reinforced composite materials cracks always start in the matrix and tend to advance parallel to the fiber direction. This behavior is the opposite of that observed in tests carried out on homogeneous isotropic specimens.

The mechanical properties of each phase (matrix and fiber) are summarized in Tables 1 and 2.

An incremental analysis considering 30 displacement increments was performed. The total displacement imposed at the top of the specimen was 0.385 mm.

Fig. 7a shows the deformation of the specimen in the final state. These figures present a displacement amplification factor of 50 illustrating the most important phenomena obtained in the analysis. In this type of fiber reinforced composite material four cracks start in the notch root and progress parallel to the longitudinal axis of the specimen coincident with the reinforcement direction. The origin of two of the cracks can be appreciated in Fig. 7a. They start in the notch root and spread in the direction of the longitudinal axis.

In Fig. 7b contours of the displacements norm is presented. It is observed that in the central area of the specimen the displacement field presents a soft gradient, with four areas clearly distinguished where displacement gradients are high. These areas begin in the root of each notch and progress parallel to the longitudinal axis of the specimen, coincident with the reinforcement direction.
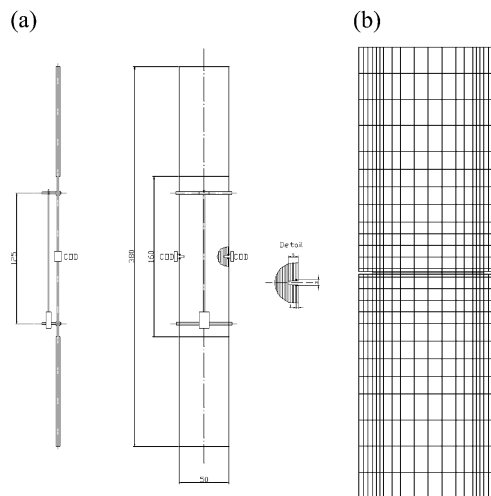
(a)   (b)

Fig. 6. Specimen geometry. Dimensions, mesh and detail of the central part.

Table 1
Properties of epoxi resin

Young modulus	14,715 MPa
Poisson coefficient	0.325
Yield stress	43,323 MPa
Post yield behavior law	Exponential with softening
Fracture energy	5 N/m
V_m	52.5%

Table 2
Properties of carbon fiber

Young modulus	239,551 MPa
Poisson coefficient	0.0
Yield stress	300 MPa
Post yield behavior law	Linear with hardening
V_f	47.5%
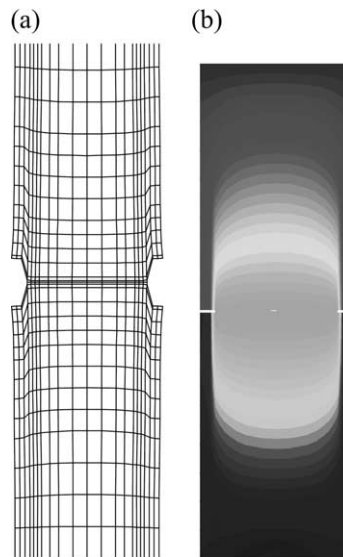
Fig. 7. Test of T300/914C specimen with 0° fiber angle. (a) Deformation (amplified 50 times) and (b) contours of displacement norm.

The equivalent plastic strain contours in the composite are plotted in Fig. 8d. The areas with higher straining are in the notch root due to the concentration of stresses. Plasticity effects progress in a parallel direction to the longitudinal axis of the sample.

Fig. 8e shows the plasticity levels in fibers clearly indicating the regions where the debonding phenomenon has taken place. One of the reasons of the non-linear behavior of reinforced composite materials is due to the phenomenon of crack propagation in the matrix and the relative displacement between fiber and matrix. The phenomenon of matrix cracking and debonding or slip between fibers and matrix reduces the global stiffness and leads to inelastic or not recoverable strains. This phenomenon is taken into account here by limiting the load capacity of the fibers due to the inability of the matrix to transmit the loads. More
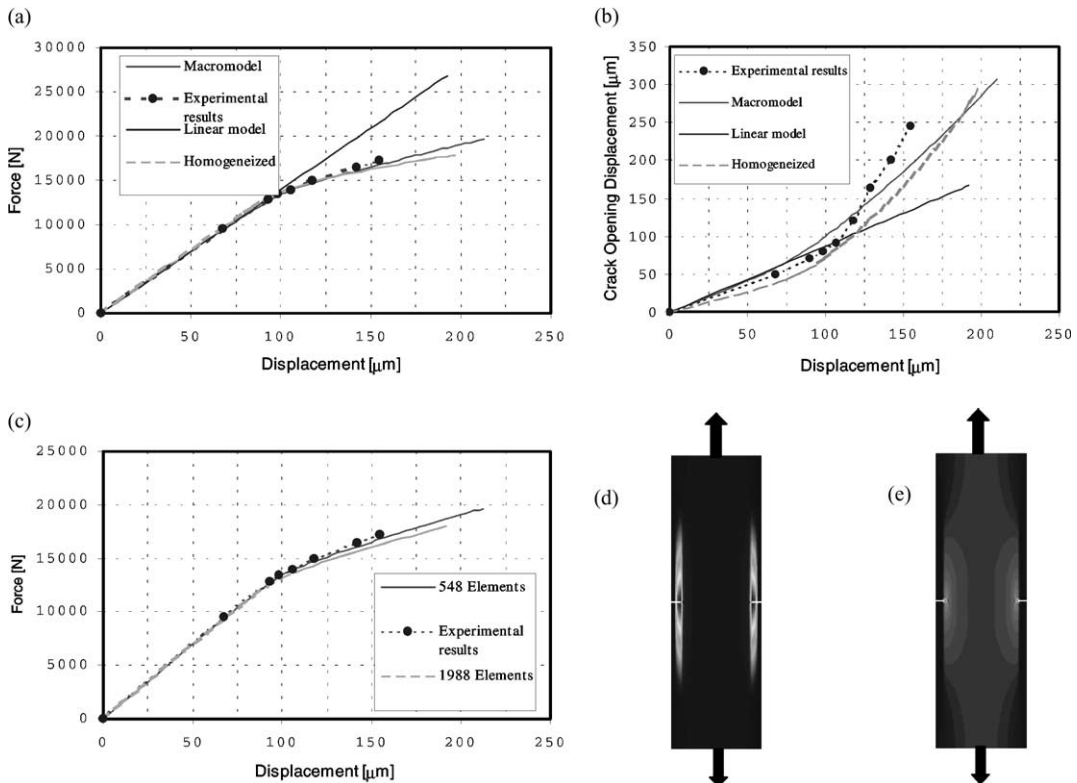
Fig. 8. Test of T300/914C specimen with 0° fiber angle. (a) Load vs. displacement, (b) COD vs. displacement, (c) load vs. displacement with different meshes at the top of the specimen, (d) equivalent plastic strain contours in the composite and (e) equivalent plastic strain contours in fibers.

details about modeling of this phenomenon are presented in Car (2000). Fig. 8 also clearly shows that cracks progress from the root of the notch, due to the concentration of stresses in this area, towards the center of the specimen. The debonding phenomenon prevents fibers reaching the maximum yield stress as the matrix is not able to transfer the load to the fiber. This also leads to a change in the slope of the load–displacement curve (Fig. 8a).

Some experimental and numerical results are compared in Fig. 8a and b. The curve in Fig. 8a shows the force vs. the displacement at the top of the specimen. A comparison between experimental results, the results obtained with the mixing theory considering a linear elastic behavior for each phase and the proposed non-linear models are presented. Results using the linear elastic model provide upper limit values.

At high load levels, a non-linear behavior is observed in experimental tests due to debonding phenomena between fibers and matrix. Numerical results detect with remarkable agreement the onset of this non-linear phenomenon. In Fig. 8b, curves relating the displacement at the top level of the specimen and the crack opening displacement (COD) in the central area are plotted (see Fig. 6).

Fig. 8b shows that the COD obtained with the homogenization method are lesser than the experimental results. The COD obtained with the macro-model is greater than the experimental results up to 125 μm of displacement at the top of the specimen. For greater displacement at the top of the specimen, the numerical results obtained with the macro-model are lesser than the experimental results.

Fig. 8c shows the load vs. displacement plot at the top of the specimen for different meshes. This figures shows that the macro model is mesh independent. In the case of the macro-micro model, mesh independence has not been proven, but there is no evidence that it exists.

5. Concluding remarks

In this work two procedures to simulate the constitutive behavior of fiber reinforced composite materials are presented. These procedures are based on two different concepts. The first one simulates the constitutive behavior considering a macroscopic approach (Mixing theory), whereas the second procedure, based on a multiscale approach (Homogenization theory), takes into account the composite material microstructure. In spite of the different nature of the procedures the obtained results show a good agreement with the experimental values. CPU time needed to solve the example and the finite element code are also different. The Homogenization theory requires a parallel code due to the large number of computations required.

Acknowledgements

Appendix A. Microstructure representation

In Fig. 9 the unit volume called cell is showed. In this figure the two phases of the material are observed: matrix and fiber. In this case the unit cell is a prism with quadrilateral section in which are contained the reinforcement phase and the matrix. In this domain, the dimensions of the fiber and matrix zones are
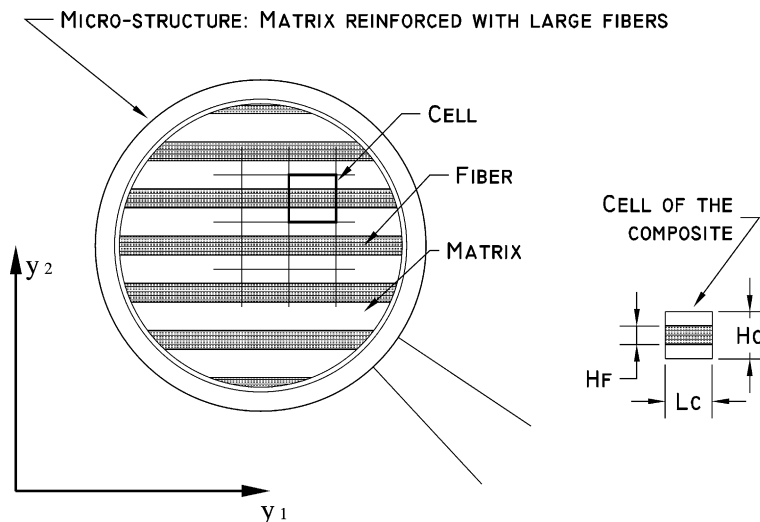

Fig. 9. Microstructure and unit cell.

Table 3
Cell dimensions

V_f	0.525
V_m	0.475
Fiber diameter (d_f) (μm)	5
Cell length (l_c) (μm)	8
Cell height h_c (μm)	6.429366
Equivalent fiber height h_f (μm)	3.053949

related to the volumetric participation of the two phases in the whole composite material. The bidimensional approximation requires that the circular section of the fiber must be replaced by a rectangular equivalent section. The dimensions of the cell, and each phase of the composite are showed in Table 3.

The unit cell is discretized with 24 quadrilateral finite element under plane stress condition. To simulate the constitutive behavior of the matrix, an exponential damage law is used (Oliver et al., 1990). The constitutive behavior of the fiber is simulated through a classical Von Mises plasticity model. All the phases in the cell are considered isotropic. The anisotropic behavior of the whole composite is obtain through the homogenization theory.

References

Ali, R., 1996. Use of finite element technique for the analysis of composite structures. Comput. Struct. 58 (5), 1015–1023.

Bensoussan, A., Lions, J.L., Papanicolaou, G.C., 1978. Asymptotic Analysis for Periodic Structures. North-Holland, Amsterdam.

Betten, J., 1981. Creep theory of anisotropic solids. J. Rheol. 25, 565–581.

Betten, J., 1988. Application of tensor functions to the formulation of yield criteria for anisotropic materials. Int. J. Plasticity 4, 29–46.

Car, E., 2000. A Continuum Constitutive Model to Simulate the Mechanical Behavior of Composite Materials. PhD Thesis, Universidad Politécnica de Cataluña.

Car, E., Oller, S., Oñate, E., 2001. A large strain plasticity model for anisotropic materials-composite material application. Int. J. Plasticity, Pergamon Press, 17 (11), 1437–1562.

Car, E., Oller, S., Oñate, E., 2000. An anisotropic elastoplastic constitutive model for large strain analysis of fiber reinforced composite materials. Computer Meth. Appl. Mech. Engng. 185 (2), 245–277.

Duvaut, G., 1976. Analyse Fontionnelle et Mécanique des Milieux Continus. In: Th. Appl. Mech. North Holland, Amsterdam, pp. 119–132.

Dvorak, G.J., Bahei-El-Din, Y.A., Wafa, A.M., 1994. Implementation of the transformation field analysis for inelastic composite materials. Comput. Mech. 14, 201–228.

Fish, J., Shek, K., Pandheeradi, M., Shephard, M., 1997. Computational plasticity for composite structures based on mathematical homogenization: theory and practice. Comput. Meth. Appl. Mech. Engng. 148, 53–73.

Geist, A., Beguelin, A., Dongarra, J., Jiang, W., Manchek, R., Sunderam, V., 1994. Parallel Virtual Machine—A Users' Guide and Tutorial for Networked Parallel Computing. Massachusetts Institute Technology.

Ghosh, S., Lee, K., Moorthy, S., 1996. Two scale analysis of heterogeneous elastic–plastic materials with asymptotic homogenization and voronoi cell finite element model. Comput. Meth. Appl. Mech. Engng. 132, 63–116.

Green, A., Naghdi, P., 1965. A dynamical theory of interacting continua. J. Engng. Sci. 3, 3–231.

Klintworth, J., Macmillian, S., 1992. In: Effective analysis of laminated composite structures. Benchmark, NAFEMS, pp. 20–22.

Lene, F., 1986. Damage constitutive relations for composite materials. Engng. Fract. Mech. 25, 713–728.

Malvern, L., 1969. Introduction to the Mechanics of a Continuous Medium. Prentice-Hall, Englewood Cliffs NJ.

Oñate, E., Oller, S., Botello, S., Canet, J., 1991. Methods for analysis of composite material structures (in spanish). Technical Report 11, CIMNE, Barcelona, Spain.

Obraztsov, I.F., Vasilev, V.V., 1982. Mechanics of Composites. MIR Publishers, Moscow.

Oliver, J., Cervera, M., Oller, S., Lubliner, J., 1990. Isotropic damage models and smeared crack analysis of concrete. Second International Conference on Computer Aided Analysis and Design of Concrete Structures.

Oller, S., Oñate, E., Miquel, J., Botello, S., 1996. A plastic damage constitutive model for composite materials. Int. J. Solids Struct. 33 (17), 2501–2518.

Ortiz, M., Popov, E., 1982a. A physical model for the inelasticity of concrete. Proc. Roy. Soc. London A 383, 101–125.

Ortiz, M., Popov, E., 1982b. Plain concrete as a composite material. Mech. Mater. 1, 139–150.

Sanchez-Palencia, E., 1980. Non-homogeneous media and vibration theory. In: Lecture Notes in Physics, vol. 127. Springer, Berlin.

Sanchez-Palencia, E., 1987. Boundary layers and edge effects in composites. In: Homogenization Techniques for Composite Media. Springer, Berlin, pp. 121–192 .

Stavrinidis, C., 1985. Employment of Pam-Fiss Bi-Phase Computer Program for the Strength Analysis and Fracture Delamination Behaviour of Composites, vol. 7. Final Synthesis Report, Technical report, European Space Agency.

Suquet, P., 1982. Plasticité et Homogénéisation. PhD Thesis, Université Pierre et Marie Curie, Paris 6.

Suquet, P., 1987. Elements of homogenization for inelastic solid mechanics. In: Homogenization Techniques for Composite Media. Spring, Berlin, pp. 193–279.

Trusdell, C., Toupin, R., 1960. The Classical Field Theories, Handbuch der Physik III/I. Springer, Berlin.

Zalamea, F., 2001. Tratamiento Numérica de Materiales Compuestos Mediante la teorí de Homogeneización. PhD Thesis, Universidad Politécnica de Cataluña.

Zalamea, F., Canet, J.M., Oller, S., 1999. Teoría de homogeneización para el análisis de materiales compuestos con estructura interna periódica. In: Abascal, R., Dominguez, J., Bugeda, G. (Eds.), Proceedings del IV Congreso de Métodos Numéricos En Ingeniería. Sociedad Española de Métodos Numéricos en Ingeniería.